Impact of diverse polarisations on clutter statistics

M. Rangaswamy

Abstract: The author addresses the impact of diverse polarisations on clutter statistics in the context of waveform diversity for multi-functional operation from a specific platform as well as for multiple sensing from multiple platforms. A key issue in this context is that of clutter mitigation via the use of diverse waveforms. Classical space–time adaptive processing (STAP) methods for radar target detection can be viewed in the context of a whiten and match filter. To this end, efficient waveforms that lend themselves for such processing are sought. The author specifically considers a statistical analysis of experimental data collected at low grazing angles to validate the fact that vertical transmit–vertical receive (VV) polarised data conform to Rayleigh scatter, whereas horizontal transmit–horizontal receive data do not. Consequently, VV data are suitable for whiten and match processing adopted in conventional radar STAP.

1 Introduction

This research is motivated by the problem of adaptive radar target detection in heterogeneous clutter scenarios. The problem is complicated by the fact that the statistics and spectral properties underlying the clutter are typically unknown. Classical adaptive signal processing methods have relied upon the use of estimated clutter covariance or clutter spectrum to devise mitigation strategies. Space–time adaptive processing (STAP) is an example of such a signal processing technique. Broadly speaking, STAP for clutter mitigation can be viewed as a process of whitening followed by matched filtering, which asymptotically attains optimality for the case where the clutter scenario conforms to Gaussian statistics under regularity assumptions. Much of the research on STAP has focused on obtaining performance close to the optimal performance by innovative design of adaptive receivers, which reduce the sample support and computational cost requirements [1–6].

An emerging new direction in this context is that of waveform diversity for improved radar performance. This approach relies upon the use of a suite of waveforms to improve radar performance while maintaining a fixed receive signal processing structure. As a result, it becomes important to determine waveforms which give rise to Gaussian clutter statistics and separate them from those waveforms which result in impulsive clutter behaviour. Clutter probability density functions (PDFs) for which $P(x > \eta) > \exp(-\eta)$ are defined to be impulsive clutter scenarios. In other words, these clutter scenarios have a tail that exceeds the order of the exponential distribution. Gaussian clutter scenarios are well suited to whiten and match processing, whereas the latter requires a modification of the waveform to produce clutter statistics which lend themselves to whiten and match processing. This paper considers a statistical analysis of clutter returns from experimental data corresponding to two different polarisation states. Experimental data collected from AFRL/SNHE experiments in a wind-roughened reservoir are used in our analysis. The radar system used for this data set employed simple pulse transmission to achieve resolution in range. The single frequency S-band carrier signal was modulated by the 100 ns duration pulse in a travelling wave tube amplifier, with no additional modulation or coding. The resulting monostatic range resolution was approximately 15 m. A 1.2 m parabolic reflector antenna with a dual-polarised feed was used both for transmitting and receiving the vertical transmit–vertical receive (VV) and horizontal transmit–horizontal receive (HH) signals. Vertical and horizontal polarisations were transmitted on alternate pulses with emitted PRF of 500 Hz. The experiments were conducted at a reservoir located in central Massachusetts. The radar system was installed in a stationary truck located near the edge of the reservoir at a ground elevation of approximately 5 m above the water. The radar antenna was mounted on a telescoping tower that was fully extended to approximately 20 m and anchored with Kevlar guy lines. Thus, the radar antenna was approximately 25 m above the water surface. Grazing angles were between 3 and 3.4° to the centres of the respective range gates. The reservoir depth in the area of the measurements was approximately 3.3 m, constituting deep water conditions for the 11 cm radar wavelength. The fetch was approximately 1.25 km, with no swell for these experiment conditions. Wind speed was 6.7 m/s, and the radar observation direction was 65° from upwind. A two-channel receiver was used to collect the vertically and horizontally polarised echoes simultaneously. The relevant system parameters are reported in Table 1. Related work on the statistical properties of clutter resulting from ocean scatter can be found in [7, 8], where the K-distributed amplitude PDF was proposed for these scenarios.

2 Problem statement

Through a detailed statistical analysis involving moment calculation [9], spectral estimation methods [10] and goodness-of-fit tests [11], it is specifically demonstrated that VV and HH give rise to clutter returns with differing statistical and spectral properties. In particular, the mean,

IEE Proceedings online no. 20050051

doi:10.1049/ip-rsn:20050051

Paper first received 8th June and in revised form 29th September 2005

The author is with the Air Force Research Laboratory/SNHE, Hanscom Air Force Base, MA, USA

E-mail: muralidhar.rangaswamy@hanscom.af.mil

REPORT DOCUMENTATION PAGE

Form Approved
OMB No. 0704-0188

1. REPORT DATE *(DD-MM-YYYY)*	2. REPORT TYPE	3. DATES COVERED *(From - To)*
01-02-2006	Journal Article	2004

4. TITLE AND SUBTITLE
Impact of diverse polarisations on clutter statistics

5a. CONTRACT NUMBER
N/A

5b. GRANT NUMBER
N/A

5c. PROGRAM ELEMENT NUMBER
62204F

6. AUTHOR(S)
Muralidhar Rangaswamy

5d. PROJECT NUMBER
4916

5e. TASK NUMBER
HE

5f. WORK UNIT NUMBER
4916HE01

7. PERFORMING ORGANIZATION NAME(S) AND ADDRESS(ES)
Electromagnetic Scattering Branch (AFRL/SNHE) Source Code: 437890
Electromagnetic Technology Division, Sensors Directorate
80 Scott Drive,
Hanscom AFB, MA 01731-2909

8. PERFORMING ORGANIZATION REPORT NUMBER
N/A

9. SPONSORING/MONITORING AGENCY NAME(S) AND ADDRESS(ES)

10. SPONSOR/MONITOR'S ACRONYM(S)
AFRL-SN-HS

11. SPONSOR/MONITOR'S REPORT NUMBER(S)
AFRL-SN-HS-JA-2004-0284

12. DISTRIBUTION/AVAILABILITY STATEMENT
APPROVED FOR PUBLIC RELEASE, DISTRIBUTION UNLIMITED.

13. SUPPLEMENTARY NOTES
ESC Public Affairs Clearance #: ESC 04-0284; Published in IEE Proc-Radar Sonar Navig., Vol. 153, No.1, Feb. 2006

14. ABSTRACT
The author addresses the impact of diverse polarisations on clutter statistics in the context of waveform diversity for multi-functional operation from a specific platform as well as for multiple sensing from multiple platforms. A key issue in this context is that of clutter mitigation via the use of diverse waveforms. Classical space–time adaptive processing (STAP) methods for radar target detection can be viewed in the context of a whiten and match filter. To this end, efficient waveforms that lend themselves for such processing are sought. The author specifically considers a statistical analysis of experimental data collected at low grazing angles to validate the fact that vertical transmit–vertical receive (VV) polarised data conform to Rayleigh scatter, whereas horizontal transmit–horizontal receive data do not. Consequently, VV data are suitable for whiten and match processing adopted in conventional radar STAP.

15. SUBJECT TERMS
STAP; diverse polarizations; waveform diversity;clutter mitigation; clutter statistics

16. SECURITY CLASSIFICATION OF: a. REPORT	b. ABSTRACT	c. THIS PAGE	17. LIMITATION OF ABSTRACT	18. NUMBER OF PAGES	19a. NAME OF RESPONSIBLE PERSON
U	U	U	UU	6	Muralidhar Rangaswamy
					19b. TELEPHONE NUMBER *(Include area code)*

Table 1: Experimental data parameters

Parameter	Value
Frequency, GHz	2.7
Pulse width, μs	0.1
PRF, Hz	250
Peak transmitted power, W	500
Range resolution, m	15

calculated as defined below for the data sets

$$\begin{aligned} \mu &= E(X) = \int_{-\infty}^{\infty} x f_X(x)\,\mathrm{d}x \\ \sigma^2 &= E[(X-\mu)^2] = \int_{-\infty}^{\infty} (x-\mu)^2 f_X(x)\,\mathrm{d}x \\ \alpha_3 &= \frac{1}{\sigma^3} E[(X-\mu)^3] = \frac{1}{\sigma^3}\int_{-\infty}^{\infty} (x-\mu)^3 f_X(x)\,\mathrm{d}x \\ \alpha_4 &= \frac{1}{\sigma^4} E[(X-\mu)^3] = \frac{1}{\sigma^4}\int_{-\infty}^{\infty} (x-\mu)^4 f_X(x)\,\mathrm{d}x \\ d^{-2} &= \frac{\sigma^2}{\mu^2} \end{aligned} \tag{1}$$

where $f_X(x)$ is the PDF of the random variable X. However, while dealing with measured data, the ensemble averages defined in (1) are unknown. Consequently, these quantities are replaced by their corresponding sample moments [11]. Specifically, it is shown that VV data conform to Rayleigh scatter, thereby lending itself to whiten and match processing. However, HH data tend to be highly impulsive. Details of our approach are described in Section 3. The experimental data consist of 7500 radar returns from three range bins corresponding to VV and HH data, respectively. A covariance function estimate of the VV and HH data sets is performed first. The covariance function estimate is given by [10]

$$\begin{aligned} \hat{C}_{xx} &= \frac{1}{N-k}\sum_{i=0}^{N-k-1} [x(n)-\hat{\mu}][x^*(n+k)-\hat{\mu}^*] \\ \hat{\mu} &= \frac{1}{N}\sum_{i=1}^{N} x(i) \end{aligned} \tag{2}$$

The covariance function estimate yields the decorrelation time for VV and HH data sets. The decorrelation time is defined to be the number lags in which the normalised covariance function decays from its maximum value of unity to 0.1. Specifically, the VV data is found to decorrelate after 15 lags, whereas the HH data decorrelates after ten lags. This information is used to select uncorrelated samples from the VV and HH data sets, respectively, for further statistical analysis. In practice, it may not be possible to have the luxury of a large number of statistically independent identically distributed samples because of system considerations such as bandwidth and fast scanning arrays. In these instances, the analysis has to be modified somewhat to account for the data starved scenarios. However, for the analysis in this paper, moderate to large number of clutter samples were available, which enabled the selection of uncorrelated clutter data. This allows us to undertake a statistical analysis of the measured data. Sample moments of the data (mean, variance, skewness, kurtosis and inverse defection) [12] are calculated to validate the findings of our statistical analysis.

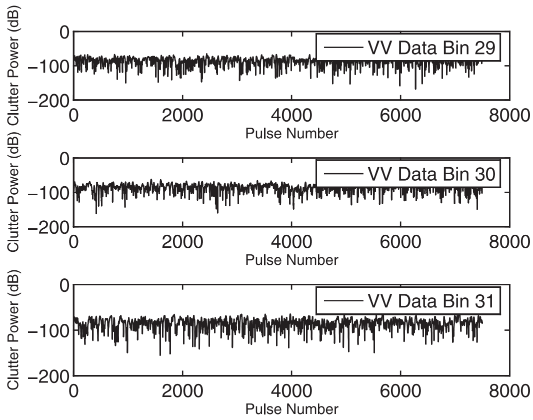

Fig. 1 *Clutter power against time: VV data*

3 Measured data analysis

Fig. 1 shows a plot of the VV data power against time, whereas Fig. 2 depicts the plot of HH data power against time. Three range bins of data consisting of 7500 pulses corresponding to VV and HH polarisations, respectively, are plotted in Figs. 1 and 2. Figs. 3 and 4 plot the amplitude and phase histograms for VV and HH data, respectively. Observe from Figs. 3 and 4 that the HH amplitude data are more impulsive compared to the VV data, although the phase histograms of both data sets conform to a uniform phase distribution in the interval $(-\pi, \pi)$.

Fig. 5 shows the power spectral density estimate for the VV data and HH data using the periodogram. The results reveal that VV and HH data exhibit significantly different spectral properties, which is consistent with the findings of [7, 8, 13]. Fig. 6 shows the covariance function for VV and HH data. Again, it is seen that the VV and HH data decorrelate on different time scales. The decorrelation time is defined to be the number of lags of the covariance function after which the magnitude of the covariance function decays to 0.1 times its maximum value. The decorrelation time is used to select data samples that are approximately uncorrelated. Decorrelation times observed under these experiment conditions of limited fetch and light winds and at the S-band measurement frequency are greater than the 5–10 ms observed at X-band in [7, 8]. A detailed discussion of this phenomenon requires

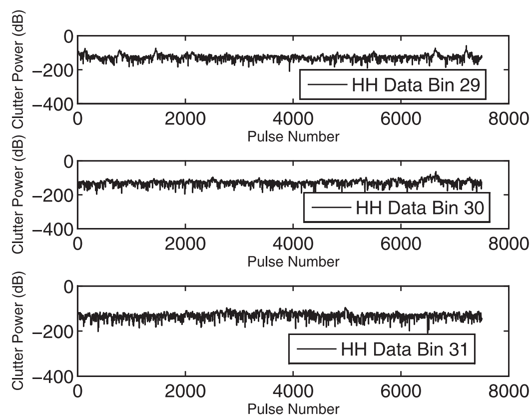

Fig. 2 *Clutter power against time: HH data*

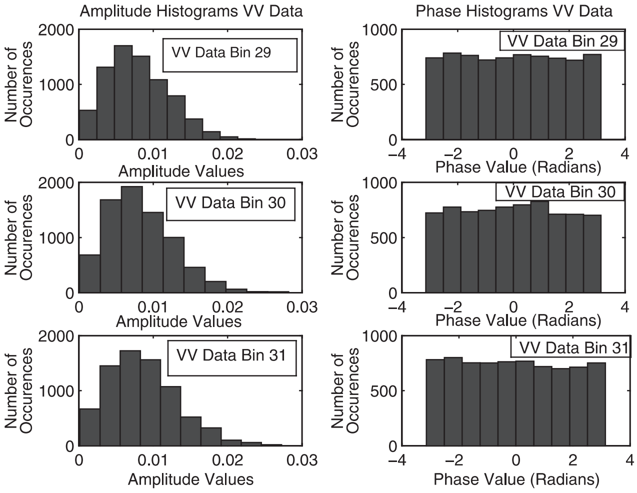

Fig. 3 *Amplitude and phase histograms for VV data*

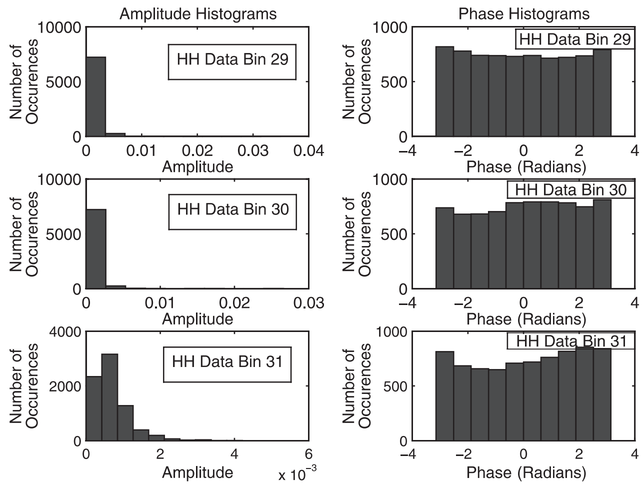

Fig. 4 *Amplitude and phase histograms for HH data*

comprehensive research pertaining to the physics of the scattering mechanism underlying the clutter, which is beyond the scope of this paper. This issue will be addressed in a future publication. The results of Fig. 4 are consistent with the findings in [14]. A Kolmogorov–Smirnov (KS) test [11] was then performed on the real and imaginary parts (I and Q components) of the VV and HH data sets to determine statistical consistency with the

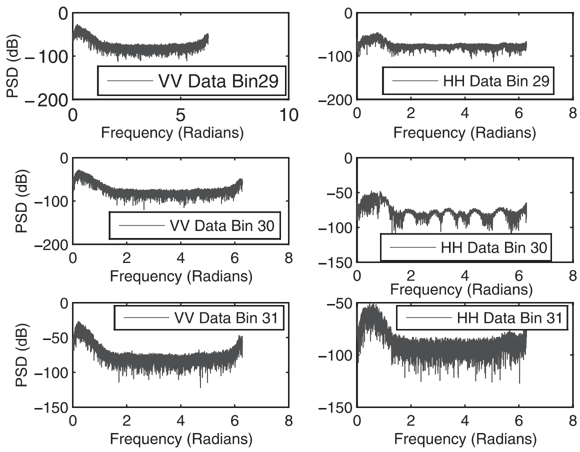

Fig. 5 *Power spectral density estimate for the VV and HH data*

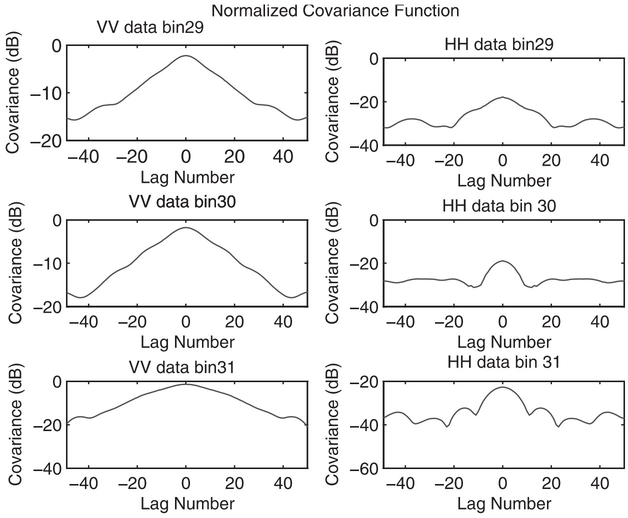

Fig. 6 *Covariance function for VV and HH data*

normal distribution. The KS test determines statistical consistency of a set of a random data with a specified PDF through a statistical hypothesis test of the form:

H_0: Data are consistent with the specified PDF

H_1: Data are not consistent with the specified PDF.

Any desired PDF may be chosen for the specified PDF under the H_0 hypothesis. For the purpose of this paper, determining statistical consistency of the data with Rayleigh scatter is of interest, which corresponds to the Gaussian PDF for the in-phase and quadrature components of the complex data. Consequently, when dealing with statistics of the scattered power, the statistical consistency of the scattered power with the exponential distribution is concerned. For convenience of analysis, the complex data sets are normalised to have zero mean and unit variance. This is accomplished by estimating the sample mean and sample variance of the data. In order to complete the KS test, a specific Type-I error probability is chosen. The Type-I error is the probability of observing under H_0 a sample outcome at least as extreme as the one observed [11] and hence provides the smallest level at which the observed sample statistic is significant. The Type-I error chosen for this paper is 0.05. The real and imaginary parts indicated statistical consistency with the normal distribution at a 5% significance level. On the other hand, real and imaginary parts of the HH data did not indicate statistical consistency with the normal distribution at a 5% significance level. The results of the KS test for the real and imaginary parts of the VV data are presented in Fig. 7. In particular, the theoretical cumulative distribution function (CDF) and empirical data CDF for the real and imaginary parts of the VV data are shown in Fig. 7. The results demonstrate excellent agreement between the theoretical CDF corresponding to the standard normal (Gaussian) distribution and empirical CDFs in all cases. As a result, the VV data sets conform to Rayleigh scattering characteristics. Corresponding results for HH data are shown in Fig. 8. In all cases for the HH data, the KS test rejected the null hypothesis at a 5% significance level. The results of Figs. 7 and 8 confirm the Rayleigh scattering characteristics of VV data, while showing that the HH data depart from Rayleigh scatter and are thus more impulsive. The statistics of the scattered power corresponding to VV and HH data are then examined. The results pertaining to range bins 29–31 are

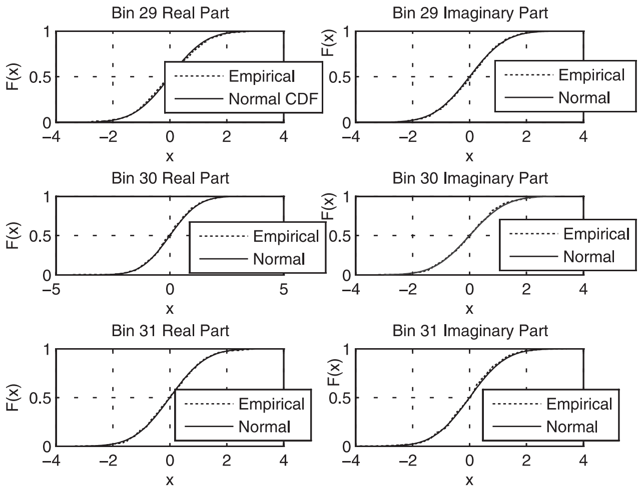

Fig. 7 *Results of the KS test for VV data*

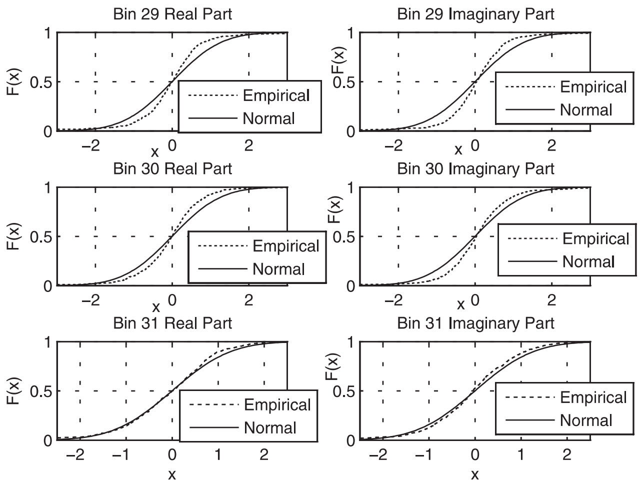

Fig. 8 *Results of the KS test for HH data*

presented in Figs. 9 and 10. First, the scattered power statistics of VV and HH data for conformance with Rayleigh scatter are tested. This is accomplished by undertaking a KS test of the scattered power data with the standard exponential distribution, whose PDF and CDF are given by

$$f_R(r) = \exp(-r), \quad r > 0$$
$$F_R(r) = 1 - \exp(-r), \quad r > 0 \tag{3}$$

The mean and variance corresponding to the exponential distribution are given by

$$E(R) = \int_0^\infty r \exp(-r)\,\mathrm{d}r = 1$$
$$\sigma_R^2 = E(R^2) - [E(R)]^2 = \int_0^\infty r^2 \exp(-r)\,\mathrm{d}r - 1 = 1 \tag{4}$$

Consequently, the inverse defection for the exponential distribution is given by

$$d^{-2} = \frac{\sigma_R^2}{[E(R)]^2} = 1$$

Thus, the inverse defection is a valuable metric for detecting departures from Rayleigh scatter. In particular, values of $d^{-2} \gg 1$ correspond to deviation from Rayleigh scattering behaviour. Furthermore, the skewness of the exponential PDF is 2. Therefore large deviations of the skewness from

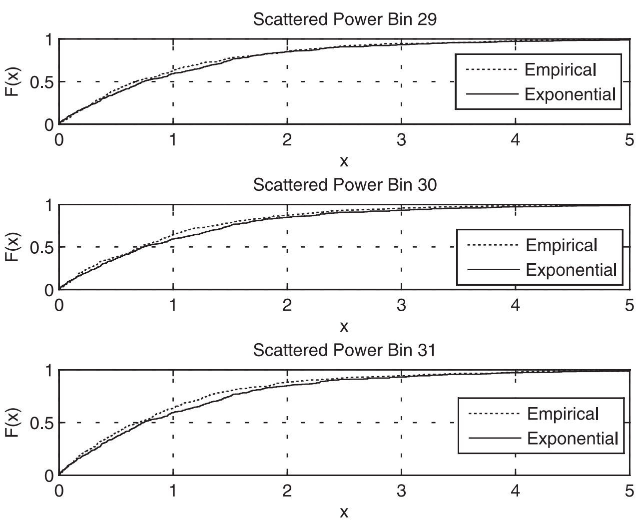

Fig. 9 *KS test results for VV data power*

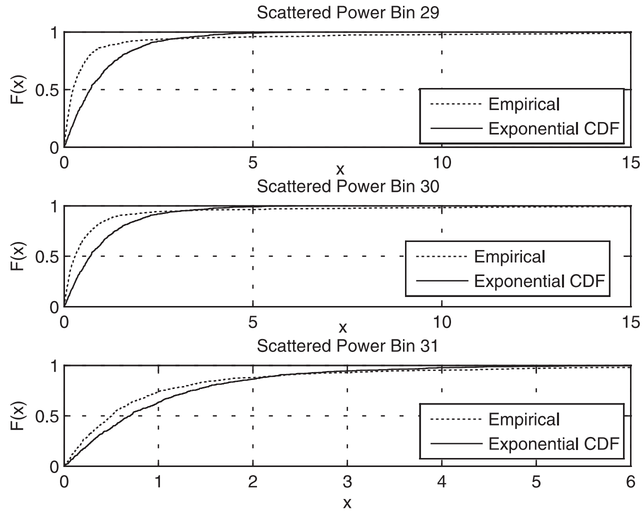

Fig. 10 *KS test results for HH data power*

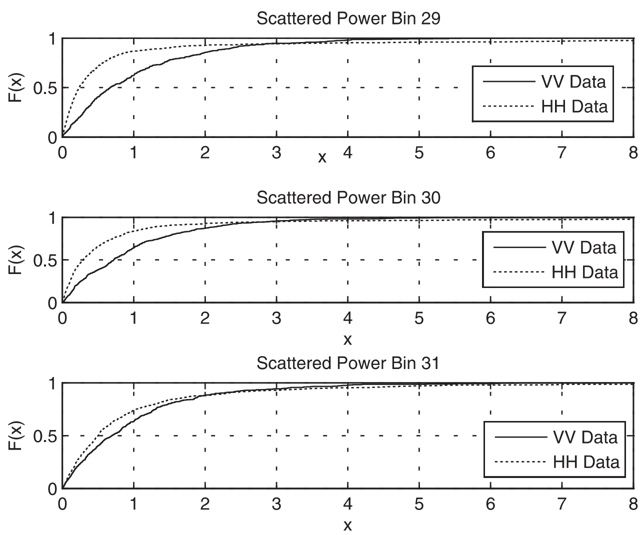

Fig. 11 *KS test results for VV and HH data power*

Table 2: Moment calculations: VV data

Moment	Bin 29	Bin 30	Bin 31
μ	0.8×10^{-4}	0.88×10^{-4}	0.96×10^{-4}
σ^2	0.58×10^{-8}	0.82×10^{-8}	0.98×10^{-8}
α_3	0.5	0.70	0.68
α_4	2.8	3.5	3.3
d^{-2}	0.91	1.05	1.06

Table 3: Moment calculations: HH data

Moment	Bin 29	Bin 30	Bin 31
μ	0.2205×10^{-5}	0.1725×10^{-5}	0.0712×10^{-5}
σ^2	0.24×10^{-9}	0.12×10^{-9}	0.002×10^{-9}
α_3	6.95	6.99	2.05
α_4	139.86	116.05	9.76
d^{-2}	50.23	39.07	3.11

2 correspond to a departure from the Rayleigh scattering behaviour. Finally, it can be shown for the normal distribution that the kurtosis is 3. Therefore data exhibiting kurtosis greater than 3 are representative of non-Rayleigh scattering phenomena.

For VV data, the null hypothesis (that the scattered power data conform to the exponential distribution) could not be rejected at a 0.05 significance level. The theoretical and empirical CDFs plotted in Fig. 9 show excellent agreement as evidenced by the KS test. Fig. 10 shows a similar plot of the empirical and theoretical CDFs of the scattered power for HH data. In this instance, the KS test rejected the null hypothesis at a 0.05 significance level for all cases. Finally, a double version of the KS test was used to determine whether the VV and HH data share the same PDF. The null hypothesis that the two data sets have the same PDF was rejected by the KS test at a 0.05 significance level for each range bin. The empirical CDFs for the VV and HH data sets from range bins 29–31 are plotted in Fig. 11. These results were further validated by moment calculations, which confirmed the findings of Figs. 5–9. The moment calculations for VV and HH data sets are summarised in Tables 2 and 3. The mean, variance, skewness and inverse deflection pertain to the scattered power, whereas the kurtosis is calculated for the real and imaginary parts of the complex data. However, the table reports only the calculation of the real part since the imaginary part has identical kurtosis as the real part.

4 Conclusions

This paper presents a statistical analysis of measured data from experiment to analyse the impact of diverse waveforms on clutter statistics. For this purpose, data corresponding to three range bins with VV and HH polarisations were processed. Statistical analysis of the data showed that the VV data and the HH data had drastically differing statistical and spectral properties. Furthermore, VV data were found to conform to Rayleigh scatter, whereas HH data exhibited an impulsive behaviour. Future work will involve the design of suitable transformations on the transmit waveform to have clutter returns which conform to Rayleigh scatter. Thus VV data lend itself to whiten and match processing adopted in conventional radar STAP. However, HH data do not lend itself to such processing.

5 Acknowledgments

This work was supported by the Air Force Office of Scientific Research (AFOSR) under Project 2304IN, by in-house research efforts at the Air Force Research Laboratory. The author is grateful to Dr. W.G. Stevens of the Air Force Research Laboratory for providing the measured data used in this analysis. Portions of this paper were presented at the First International Conference on Waveform Diversity and Design, Edinburgh, UK, November 2004.

6 References

1 Reed, I., Mallett, J., and Brennan, L.: 'Rapid convergence rate in adaptive arrays', *IEEE Trans. Aerosp. Electron. Syst.*, 1974, **AES-10**, pp. 853–863

2 Robey, F., Fuhrmann, D., Kelly, E., and Nitzberg, R.: 'A CFAR adaptive matched filter detector', *IEEE Trans. Aerosp. Electron. Syst.*, 1992, **28**, pp. 208–216

3 Kraut, S., Scharf, L.L., and McWhorter, L.: 'Adaptive subspace detectors', *IEEE Trans. Signal Process.*, 2001, **49**, pp. 1–16

4 Rangaswamy, M., Lin, F., and Gerlach, K.: 'Robust adaptive signal processing methods for heterogeneous radar clutter scenarios', *Signal Process.*, 2004, **84**, pp. 1653–1665

5 Roman, J., Rangaswamy, M., Davis, D., Zhang, Q., Himed, B., and Michels, J.: 'Parametric adaptive matched filter for airborne radar applications', *IEEE Trans. Aerosp. Electron. Syst.*, 2000, **36**, (2), pp. 677–692

6 Gerlach, K.R.: 'Outlier resistant adaptive matched filtering', *IEEE Trans. Aerosp. Electron. Syst.*, 2002, **38**, (3), pp. 885–901

7 Watts, S., and Ward, K.: 'Spatial correlation in K-distributed sea clutter', *IEE Proc. F, Commun. Radar Signal Process.*, 1987, **134**, (6), pp. 526–532

8 Ward, K., Baker, C., and Watts, S.: 'Maritime surveillance radar, Part 1: Radar scattering from the ocean surface', *IEE Proc. F, Radar Signal Process.*, 1990, **137**, (2), pp. 51–62

9 Papoulis, A.: 'Probability, random variables and stochastic processes' (McGraw-Hill, New York, 1991)

10 Marple, S.: 'Digital spectral analysis with applications' (Prentice-Hall, New Jersey, 1987)

11 Rohatgi, V.K.: 'Statistical inference' (Dover Publications Inc., Mineola, New York, 2003)

12 Dudewicz, E.J., and Mishra, S.N.: 'Modern mathematical statistics' (John Wiley and Sons, New York, 1988)

13 Plant, W., Terray, E., Petitt, R.A., Jr., and Keller, W.: 'The dependence of microwave backscatter from the sea on illuminated area: correlation times and lengths', *J. Geophys. Res.*, 1994, **99**, pp. 9705–9723

14 Long, M.: 'Radar reflectivity from land and sea' (Artech House, Norwood, MA, 2001)